Functionalized organotellurium macrocycles: Tuning optical bandgap and investigation of catalytic activity

Calvin Samuel,[a] Velpula Pramod, [a] Swandhana V. S.,[a] Alexander Steiner[b*] and Viswanathan Baskar[a*]

Table S1: Crystallographic information of **Br-TAM** and **I-TAM**.

Compound	**Br-TAM**	**I-TAM**
Empirical formula	$C_{76}H_{78}Cl_6Br_2O_{14}P_2Te_4$	$C_{74}H_{76}I_2O_{14}P_2Te_4$
Formula weight	2160.24	2015.48
Temperature/K	297(1)	298
Crystal system	monoclinic	triclinic
Space group	$P2_1/n$	*P-1*
a/Å	13.3140(4)	15.0680(3)
b/Å	23.7299(7)	17.3015(6)
c/Å	14.1869(5)	19.5456(5)
α/°	90	78.761(2)
β/°	106.379(3)	81.495(2)
γ/°	90	85.877(2)
Volume/Å^3	4300.3(2)	4938.0(2)
Z	2	2
ρcalcg/cm^3	1.668	1.356
F(000)	2112.0	1952.0
Crystal size/mm^3	0.1 × 0.1 × 0.1	0.1 × 0.05 × 0.05
Radiation	MoKα (λ = 0.71073)	MoKα (λ = 0.71073)
2Θ range for data collection/°	3.706 to 54.334	3.706 to 50.054
Index ranges	-16 ≤ h ≤ 16, -29 ≤ k ≤ 29, -17 ≤ l ≤ 17	-17 ≤ h ≤ 17, -20 ≤ k ≤ 20, -23 ≤ l ≤ 23
Reflections collected	42307	79163
Independent reflections	9028 [R_{int} = 0.1116, R_{sigma} = 0.0871]	17366 [R_{int} = 0.1063, R_{sigma} = 0.0888]
Data/restraints/parameters	9028/0/473	17366/2324/844
Goodness-of-fit on F^2	0.992	0.980
Final R indexes (F)[I>2σ(I)]	R_1 = 0.0622, wR_2 = 0.1594	R_1 = 0.0549, wR_2 = 0.1411
Final R indexes (F^2) [all data]	R_1 = 0.0931, wR_2 = 0.1784	R_1 = 0.1155, wR_2 = 0.1716
Largest diff. peak/hole / e Å^{-3}	2.10/-1.26	0.60/-0.57
Completeness to θ_{max}, %	99.3	99.5

Table S2: Selected Bond lengths (Å) and Bond angles (°) of **Br-TAM**.

Br1	Te1	3.3567(8)	Te1	Br1	Te1[1]	97.441(19)
Br1	Te1[1]	3.4936(8)	Te1[1]	Br1	Te2[1]	59.828(14)
Br1	Te2[1]	3.5434(7)	Te1	Br1	Te2	61.991(16)
Br1	Te2	3.4565(8)	Te1	Br1	Te2[1]	68.805(15)
Te1	O1	1.972(4)	Br1	Te1	Br1[1]	82.559(19)
Te1	O2	2.368(4)	O1	Te1	Br1	79.65(12)
Te1	C11	2.113(7)	O1	Te1	O2	168.68(16)
Te1	C21	2.087(6)	O1	Te1	C11	88.6(2)
Te2	O1	1.983(4)	O2	Te1	Br1	107.70(12)
Te2	O31	2.353(4)	C11	Te1	Br1	164.88(18)
Te2	C31	2.101(7)	C11	Te1	O2	85.4(2)
Te2	C41	2.118(5)	C21	Te1	O2	82.58(19)
P1	O3	1.502(5)	C21	Te1	C11	97.4(2)
P1	C51	1.788(7)	O2	P1	C51	109.4(3)
P1	C57	1.810(7)	O2	P1	C57	105.3(3)
O10	C17	1.434(12)	O3	P1	O2	116.8(2)
O20	C27	1.336(13)	O3	P1	C51	108.2(3)
C31	C32	1.381(8)	Te1	O1	Te2	125.1(2)
C32	C33	1.362(11)	P1	O2	Te1	140.1(3)
C33	C34	1.389(11)	C52	C51	P1	120.0(5)
O30	C37	1.363(11)	C56	C51	P1	121.8(6)
C60	Cl1	1.810(13)	Cl2	C60	Cl1	103.0(8)
C60	Cl2	1.753(12)	Cl3	C60	Cl1	102.9(8)
C60	Cl3	1.676(11)	O10	C14	C15	114.7(8)

[1]1-X,1-Y,1-Z

Table S3: Selected Bond lengths (Å) and Bond angles (°) of **I-TAM**.

I1	Te1	3.6559(7)	Te1	I1	Te11	91.434(16)
I1	Te11	3.7738(8)	Te1	I1	Te21	65.428(14)
I1	Te2	3.6770(9)	Te1	I1	Te2	56.511(15)
I1	Te21	3.6856(8)	Te2	I1	Te11	64.339(15)
I2	Te3	3.7472(10)	I1	Te1	I11	88.566(16)
I2	Te4	3.6486(9)	O1	Te1	I11	79.84(13)
Te1	O1	1.974(5)	O1	Te1	O2	170.11(18)
Te1	O2	2.342(5)	O1	Te1	C11	88.7(2)
Te1	C11	2.113(6)	O1	Te1	C21	90.0(3)
Te2	O31	2.349(5)	C11	Te1	I1	88.99(19)
Te2	C41	2.099(13)	C11	Te1	O2	85.3(2)
Te2	C41'	2.173(17)	C21	Te1	I1	169.7(2)
O2	P1	1.481(6)	C21	Te1	I11	86.4(2)
O3	P1	1.493(5)	C21	Te1	C11	94.2(3)
O20	C27	1.438(13)	Te2	O1	Te1	124.1(2)
O20'	C27'	1.397(15)	P1	O2	Te1	135.2(3)
C31	C32	1.357(9)	P1	O3	Te21	138.0(3)
C31	C36	1.379(8)	Te4	O4	Te3	123.6(2)
C32	C33	1.408(9)	P2	O5	Te3	137.9(4)
C33	C34	1.354(9)	P2	O6	Te42	132.0(3)
P1	C121	1.728(13)	O5	P2	O6	117.6(3)
P1	C12A	1.780(18)	O5	P2	C21A	93.0(7)
O5	P2	1.490(5)	C221	P2	C21A	125.9(8)
O6	P2	1.508(6)	C22B	C221	P2	115.0(13)

[1]2-X,2-Y,-Z; [2]1-X,1-Y,1-Z

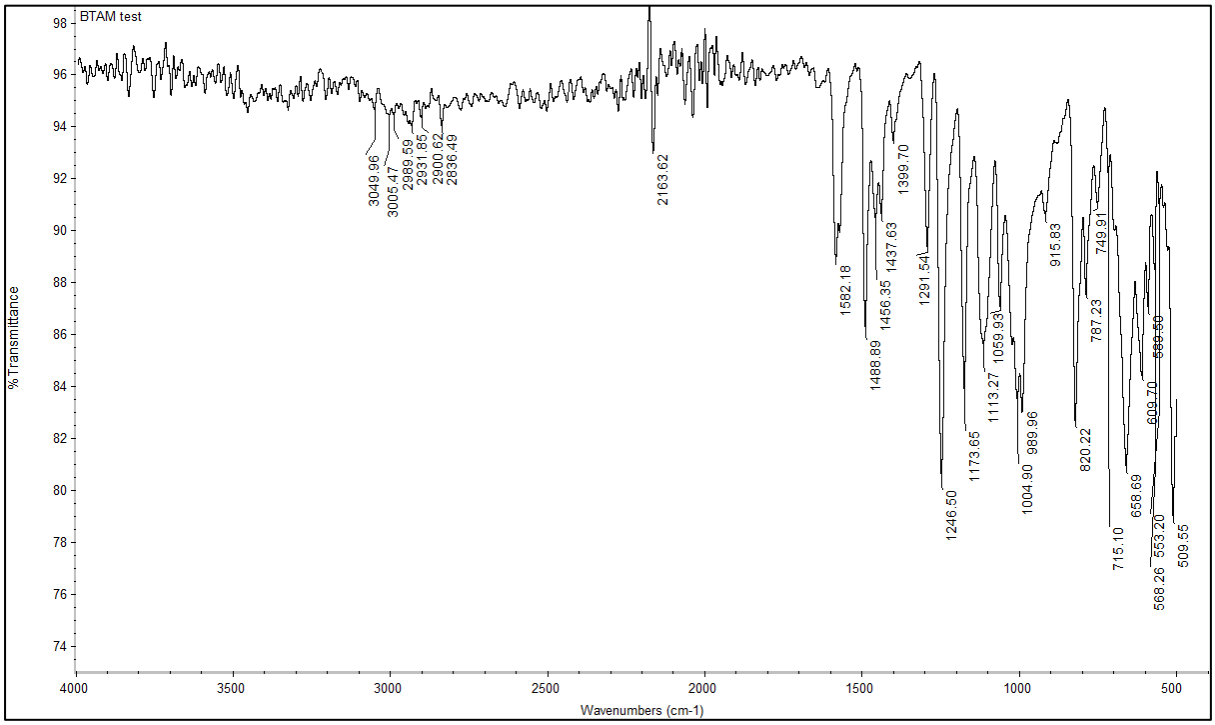

Figure S1: FTIR spectrum of **Br-TAM**.

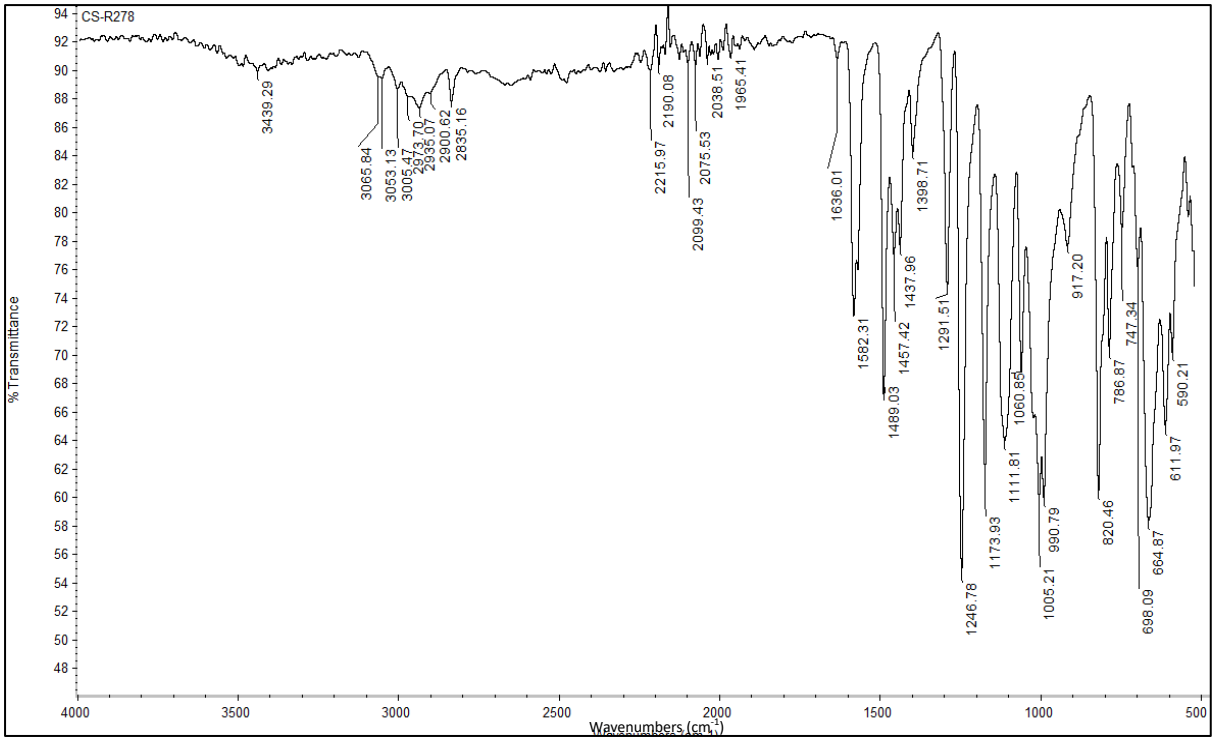

Figure S2: FTIR spectrum of **I-TAM**.

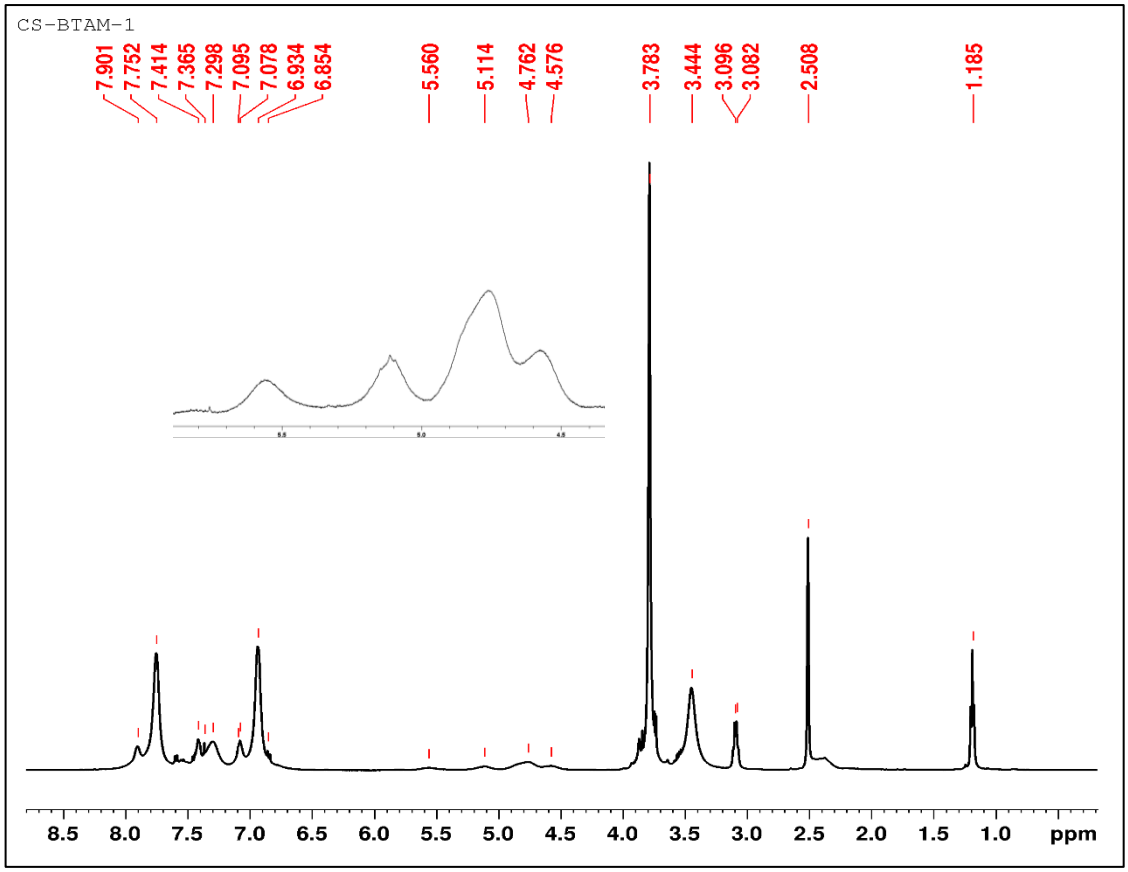

Figure S3: ^{1}H NMR of **Br-TAM** in DMSO-d$_6$.

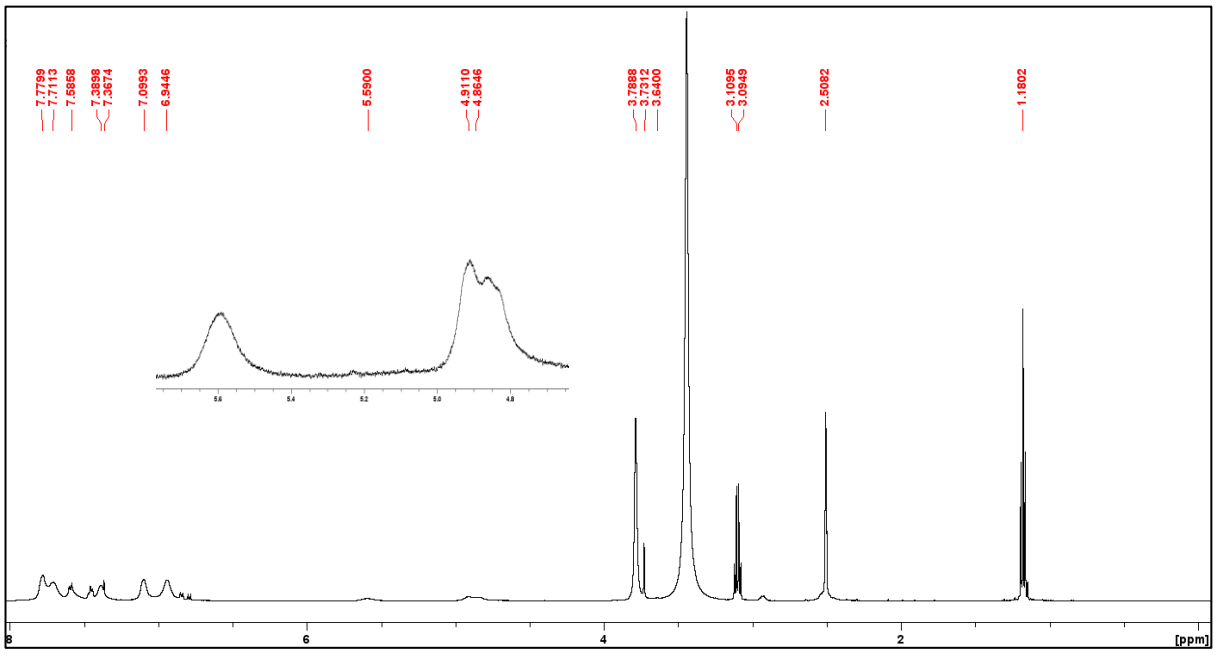

Figure S4: ^{1}H NMR of **I-TAM** in DMSO-d$_6$.

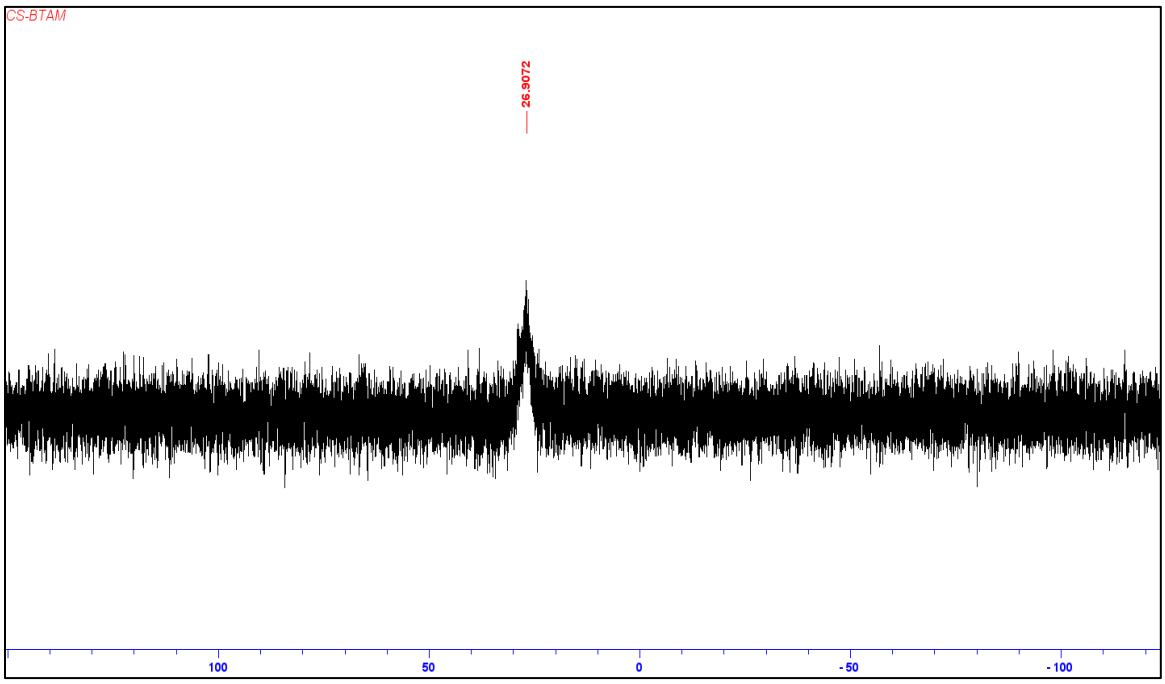

Figure S5: ^{31}P NMR of **Br-TAM** in DMSO-d_6.

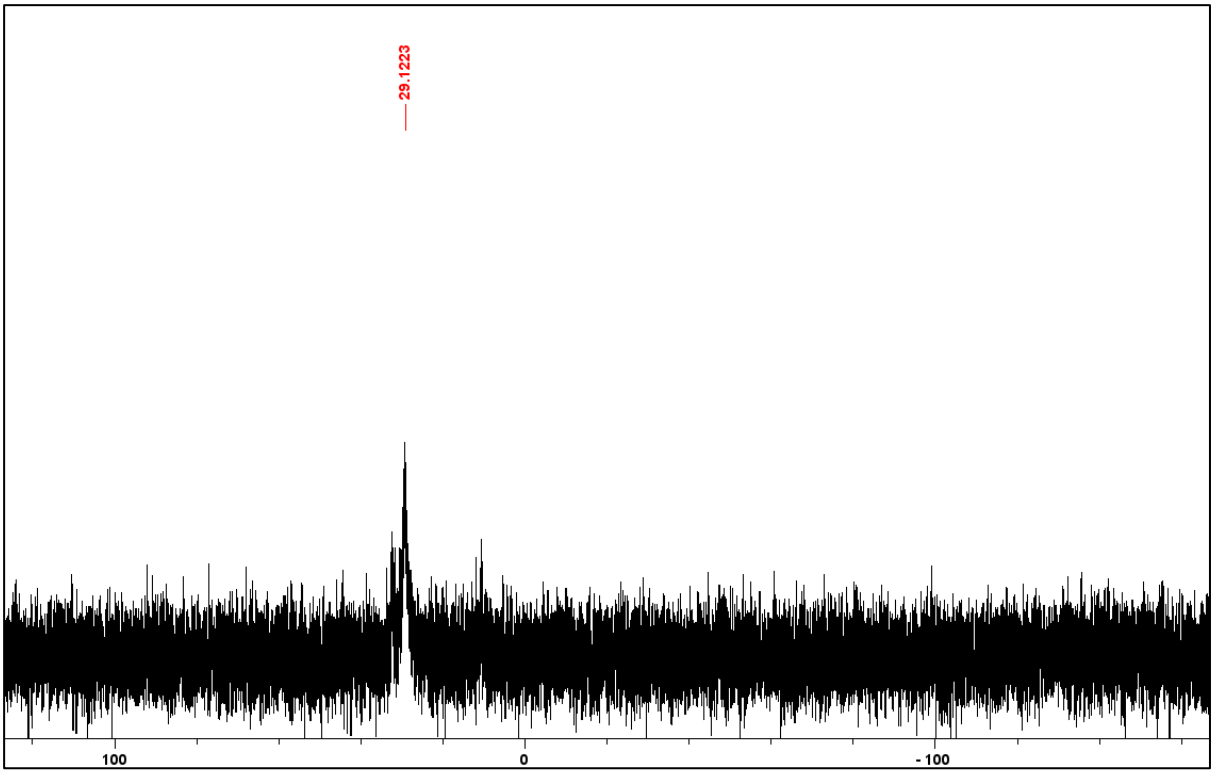

Figure S6: ^{31}P NMR of **I-TAM** in DMSO-d_6.

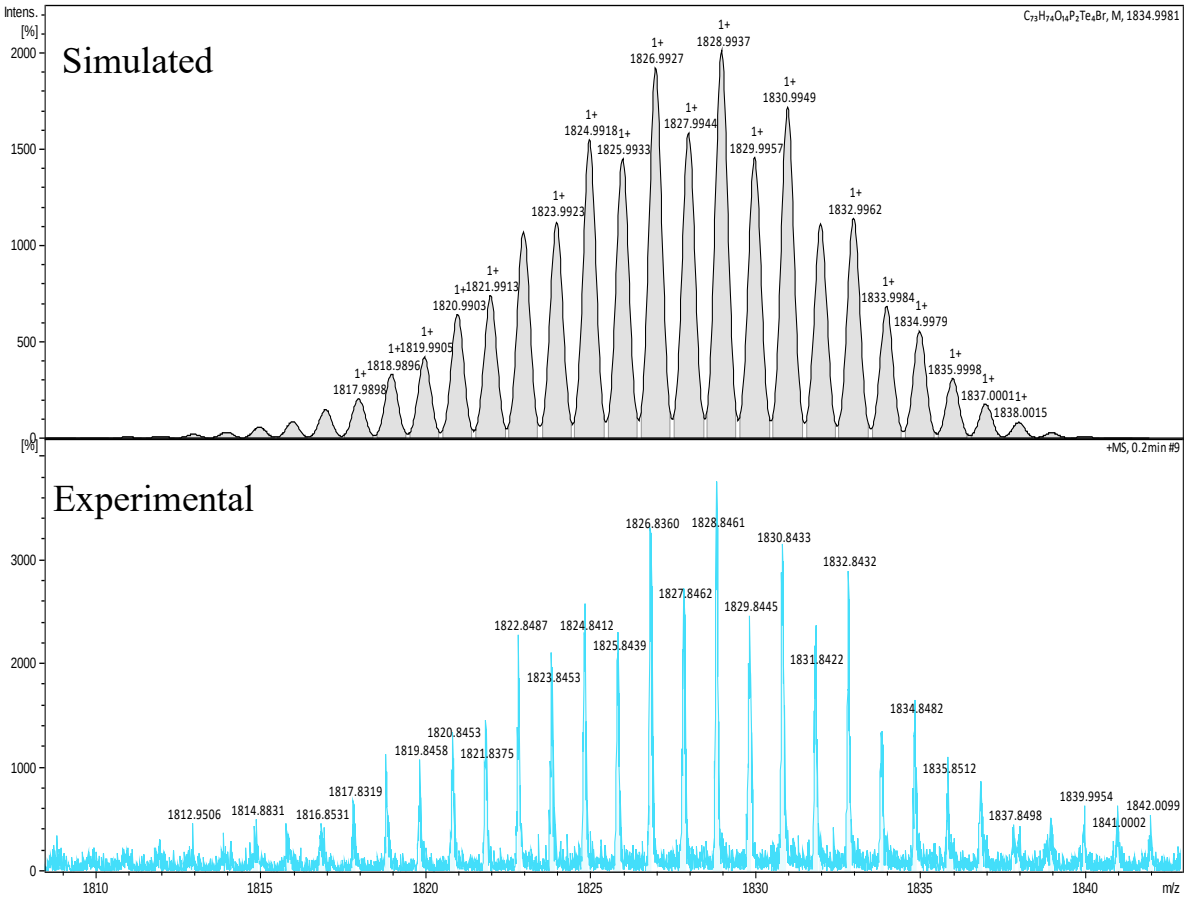

Figure S7: ESI-MS of **Br-TAM**.

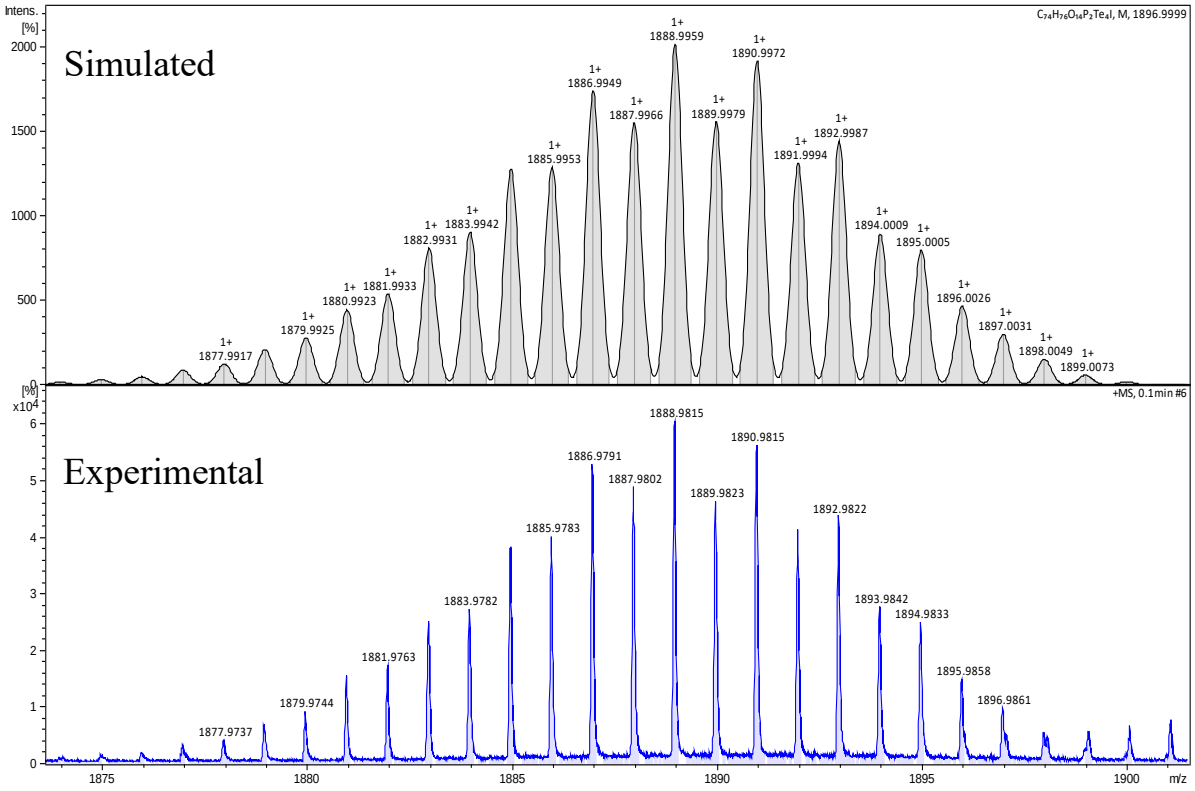

Figure S8: ESI-MS of **I-TAM**.

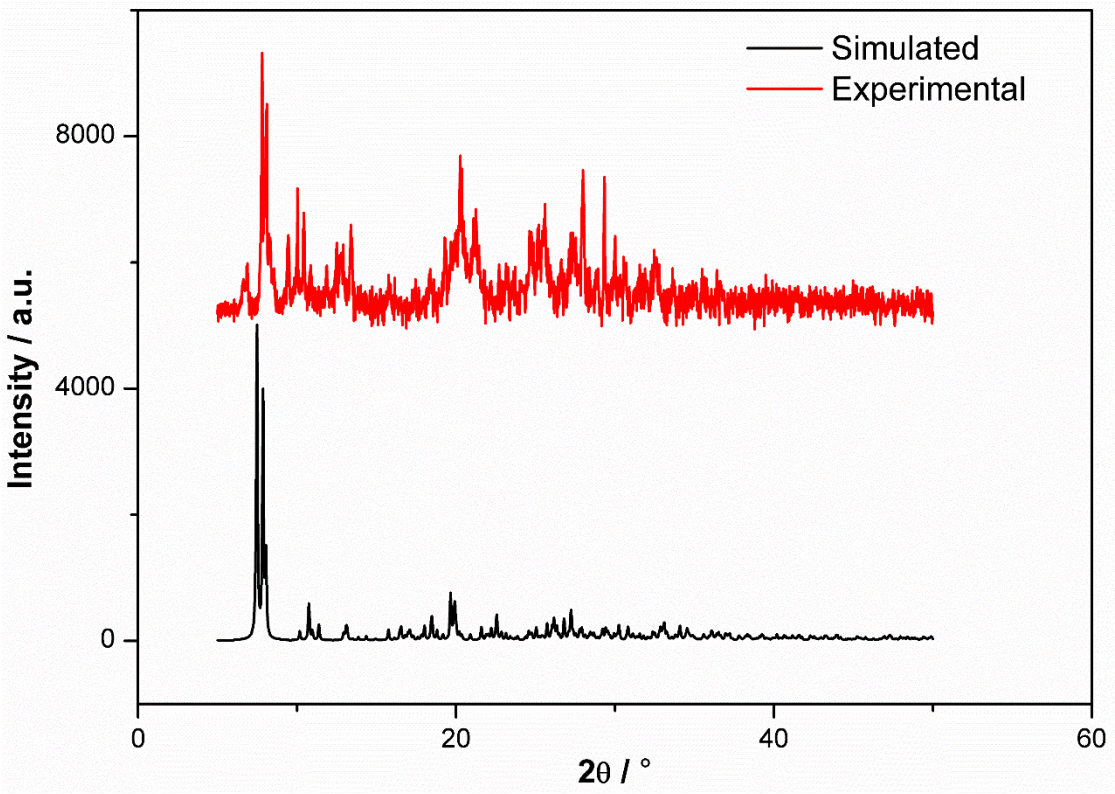

Figure S9: PXRD diffraction pattern of a bulk sample of **Br-TAM**.

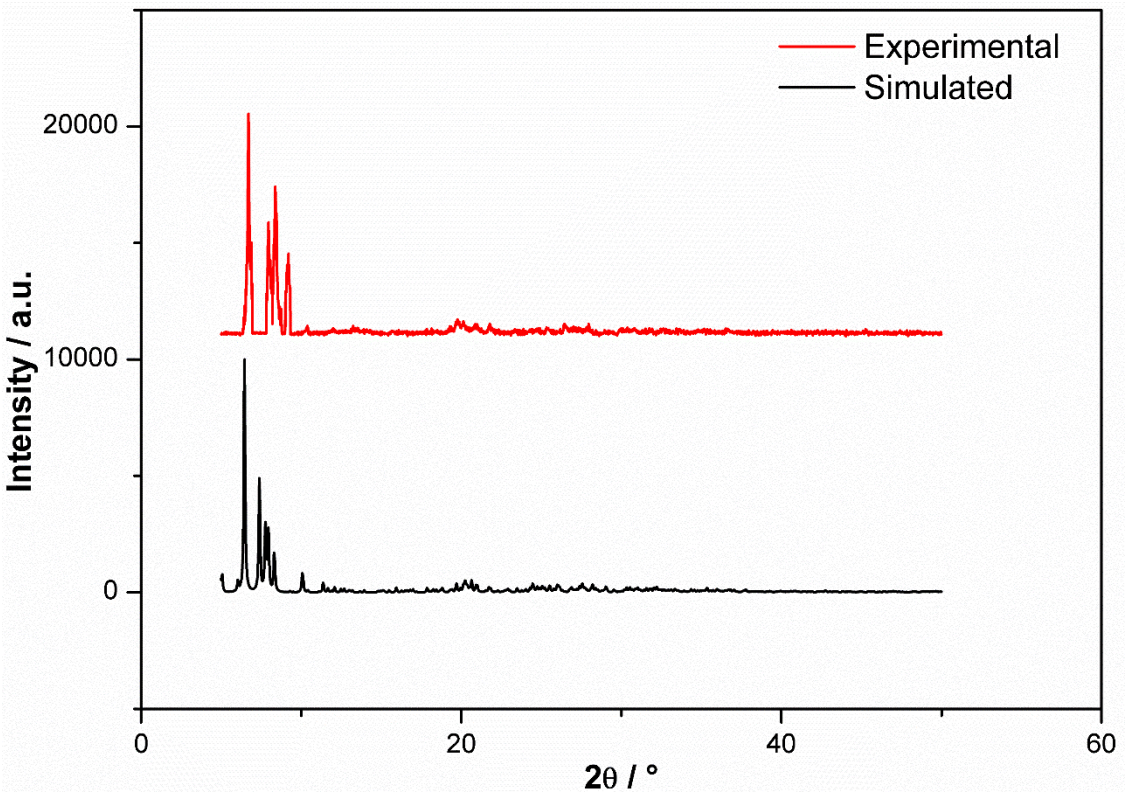

Figure S10: PXRD diffraction pattern of a bulk sample of **I-TAM**.

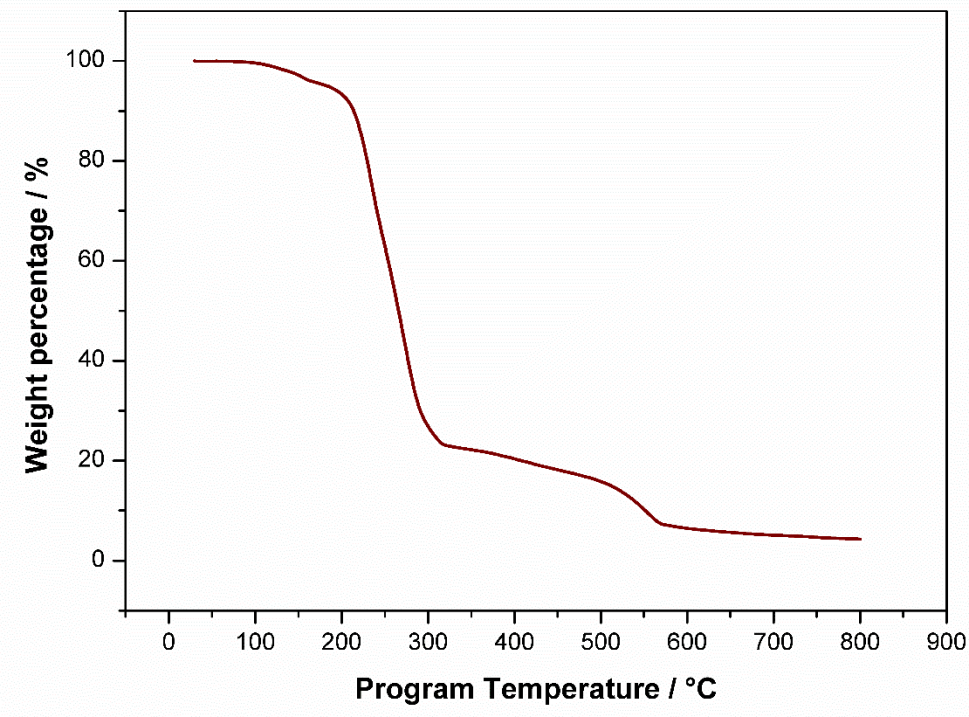

Figure S11: TGA of **Br-TAM**.

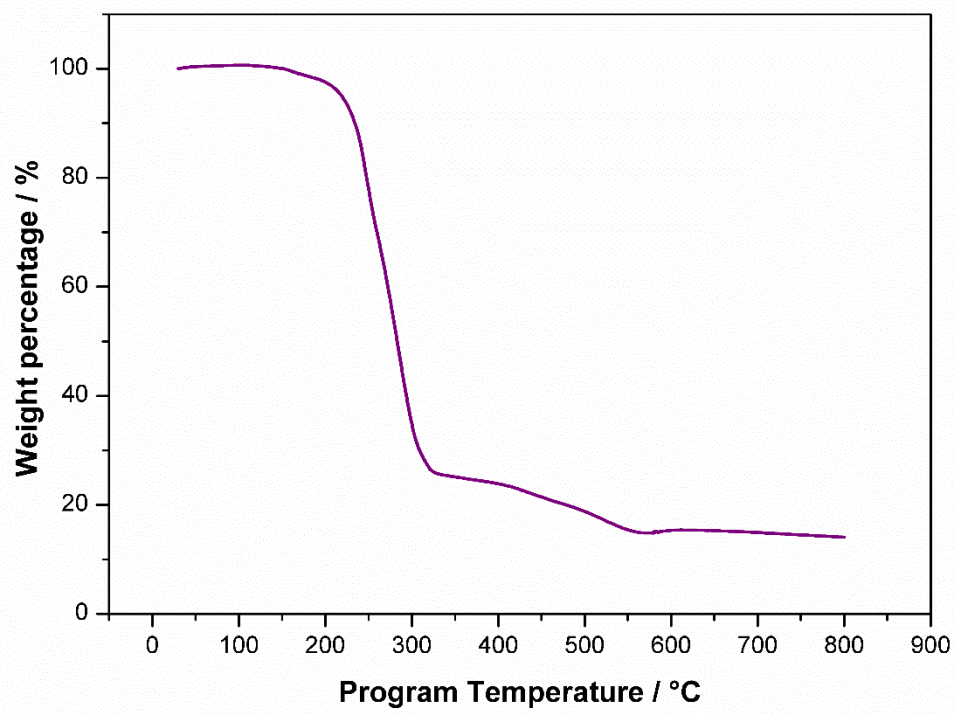

Figure S12: TGA of **I-TAM**.

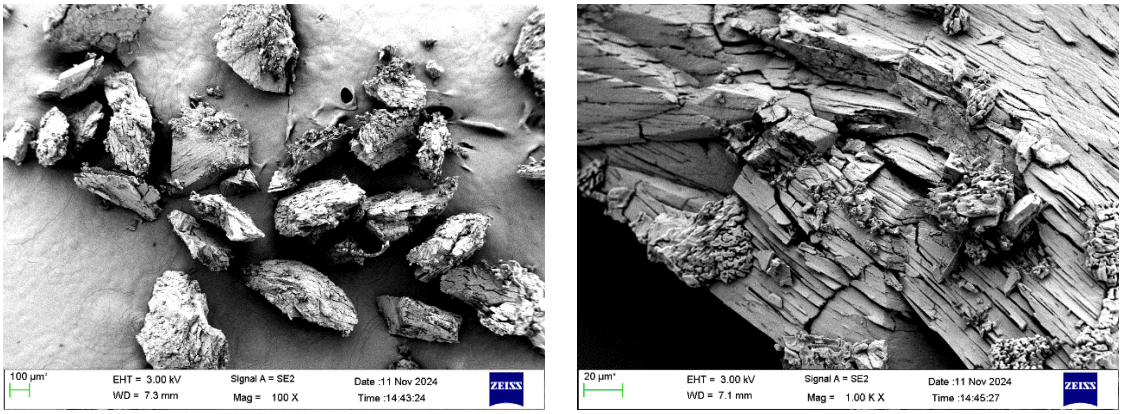

Figure S13: FESEM images of **Br-TAM**.

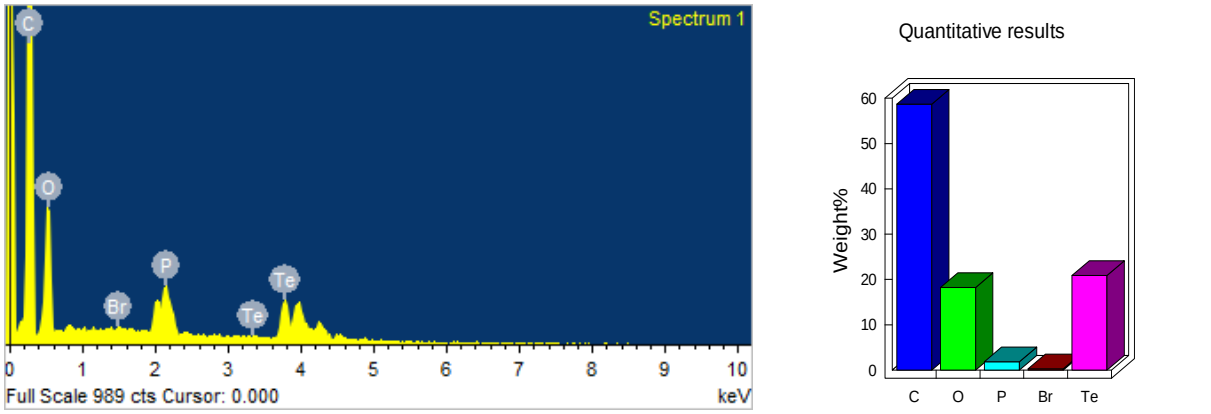

Figure S14: EDAX spectrum of **Br-TAM**.

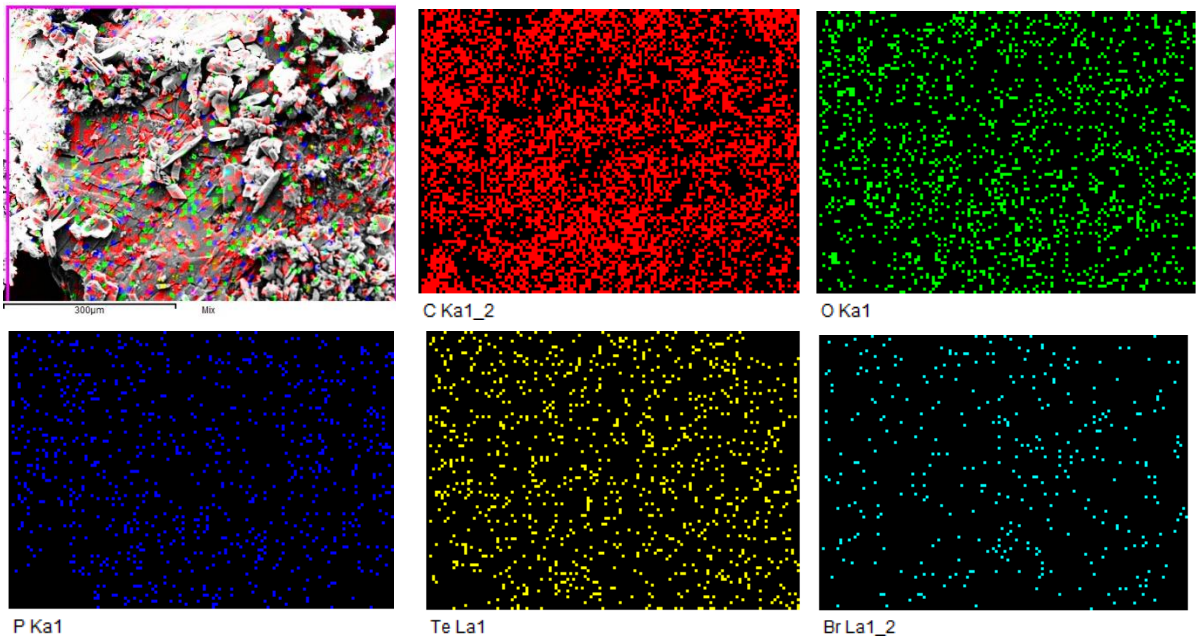

Figure S15: Elemental mapping of **Br-TAM**.

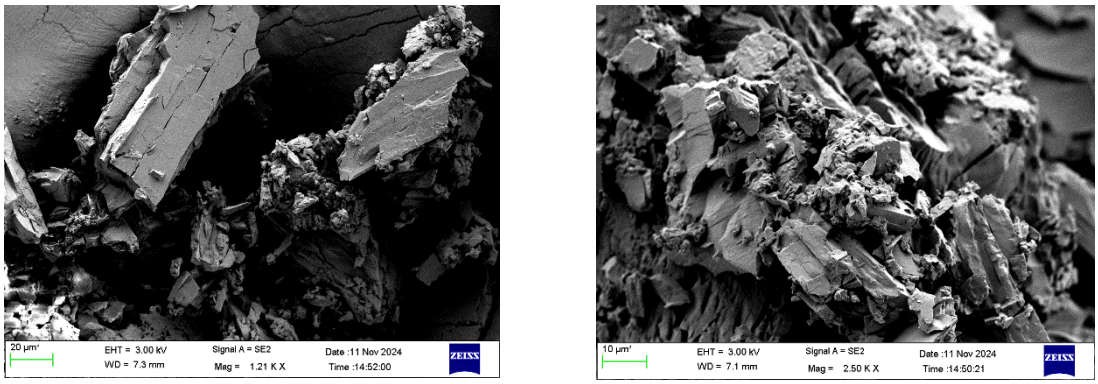

Figure S16: FESEM images of **I-TAM**.

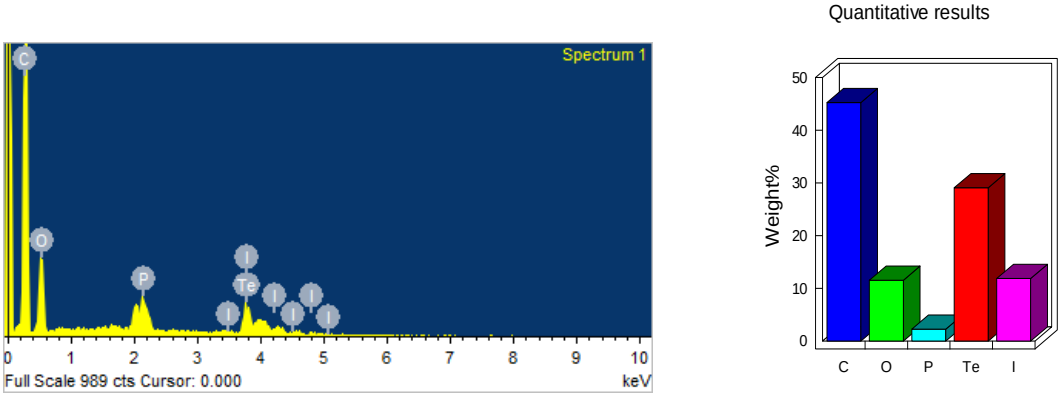

Figure S17: EDAX spectrum of **I-TAM**.

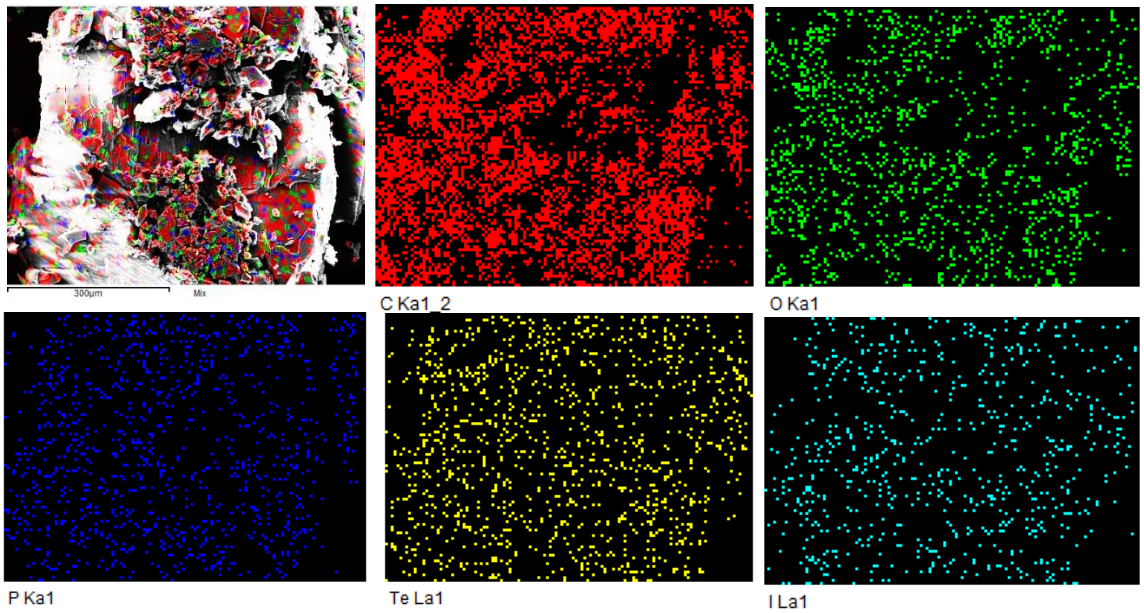

Figure S18: Elemental mapping of **I-TAM**.

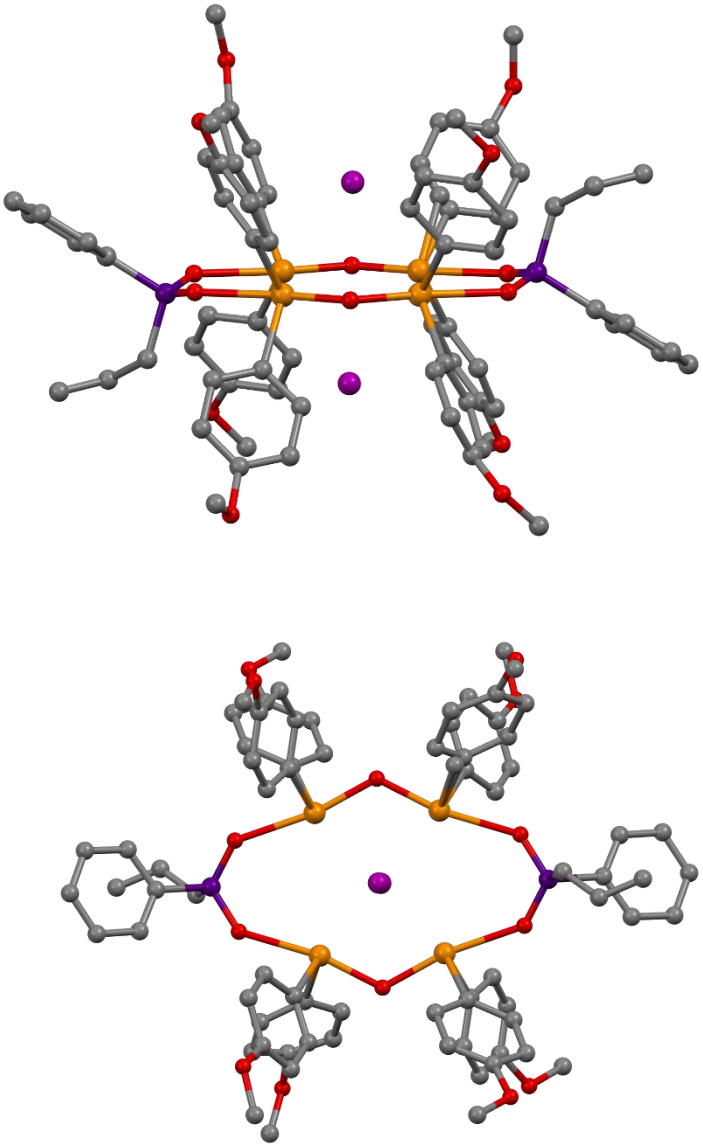

Figure S19: Structure of **I-TAM**. Hydrogens have been omitted for clarity. Colour code: Orange – Te, violet – I, purple – P, red – O, grey – C.

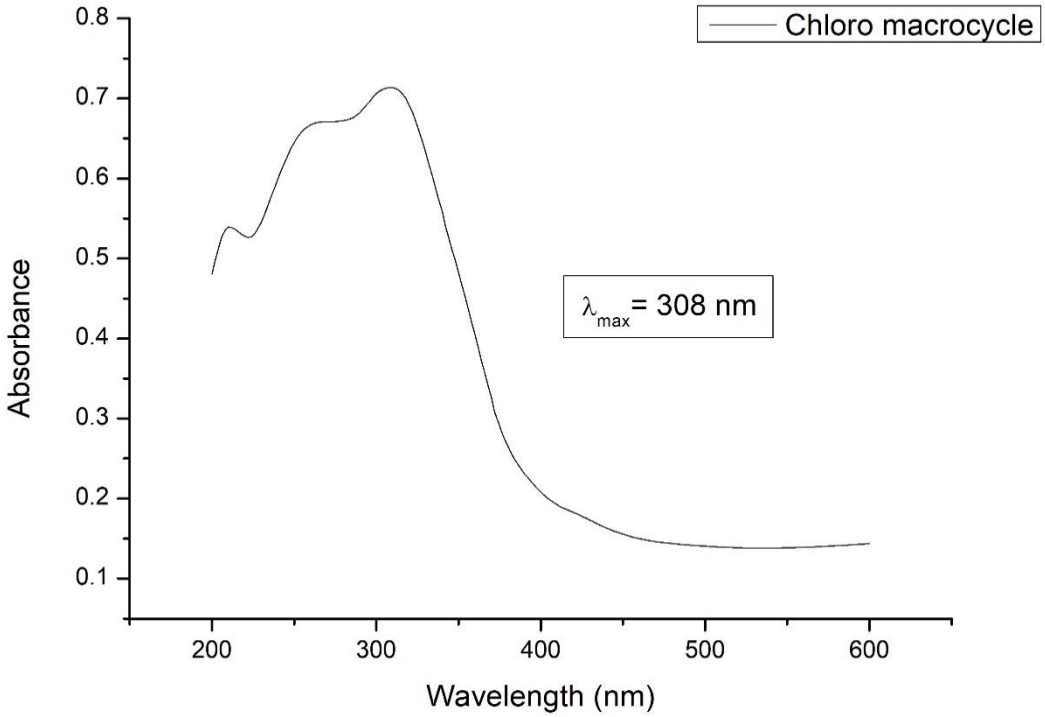

Figure S20: Solid state UV-Vis spectrum of **Cl-TAM**.

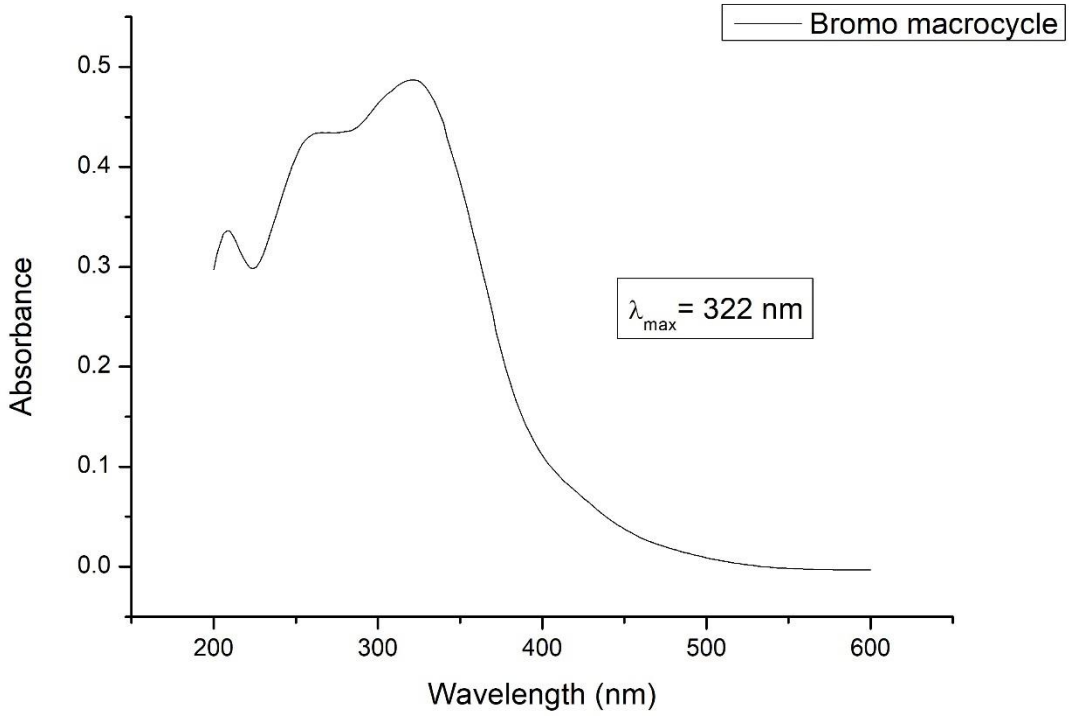

Figure S21: Solid state UV-Vis spectrum of **Br-TAM**.

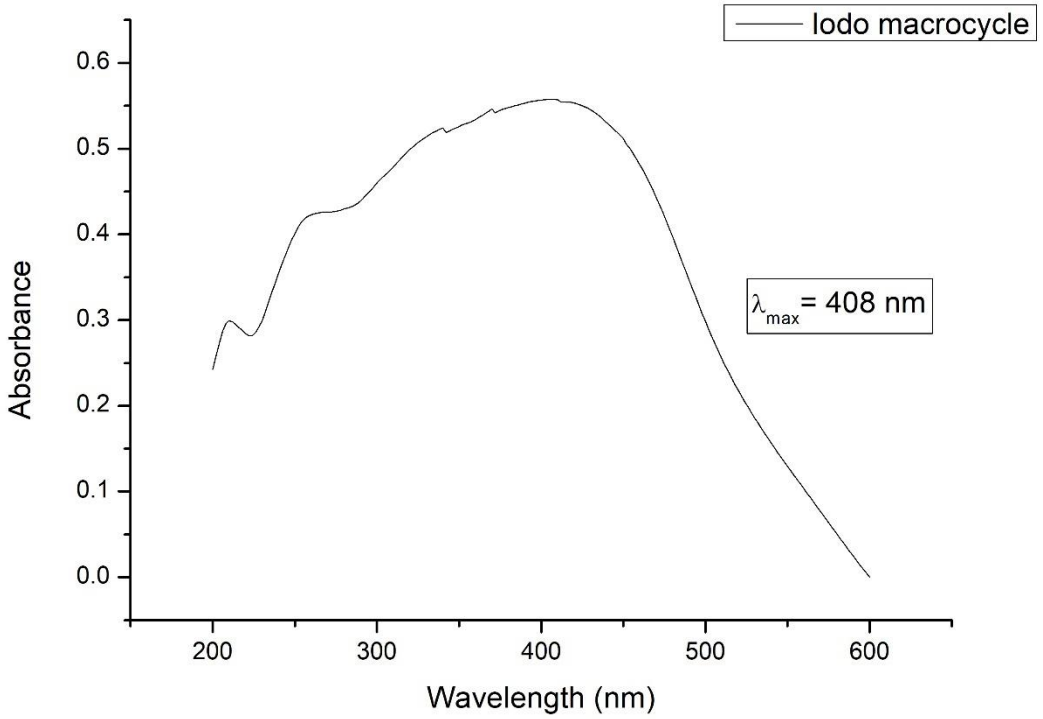

Figure S22: Solid state UV-Vis spectrum of **I-TAM**.

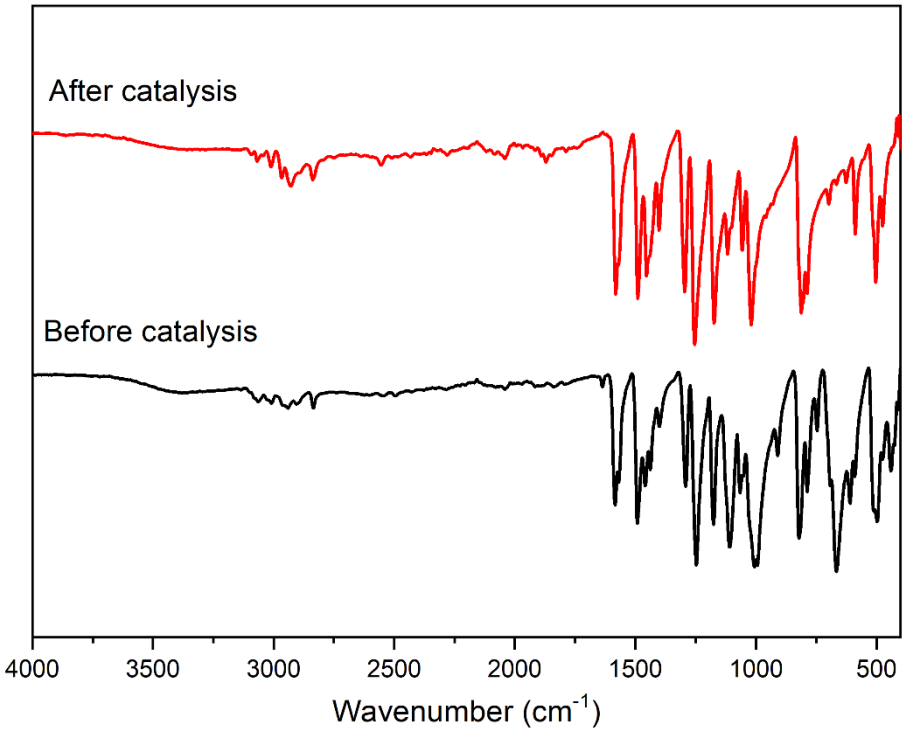

Figure S23: FTIR spectrum of **Cl-TAM** before and after catalysis.

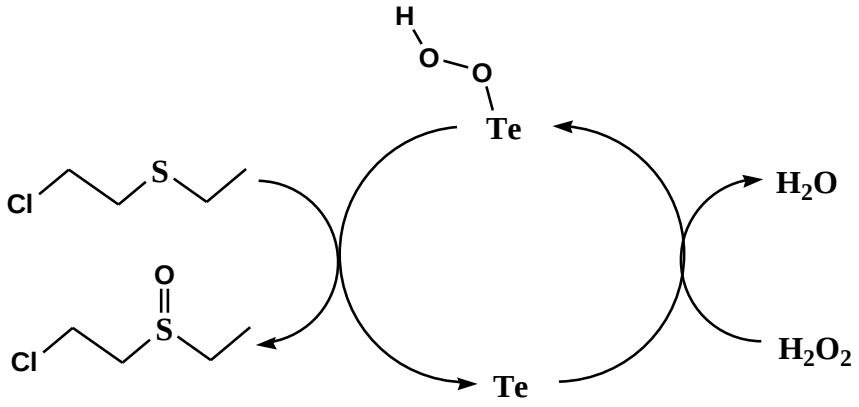

Figure S24: Plausible mechanism of CEES oxidation using tellurium macrocycle as catalysts.